

## PROMPT PHOTONS AND PARTICLE MOMENTUM DISTRIBUTIONS AT HERA

N. GOGITIDZE

*DESY, Notkestrasse 85, 22607 Hamburg, Germany*  
*E-mail: nellyg@mail.desy.de*

Recent results, obtained by the H1 and ZEUS collaborations, are presented on differential cross sections, for inclusive prompt photon production in DIS and for photoproduction of prompt photons accompanied by a hadronic jet. Also presented are cross sections of normalised scaled momentum distribution of charged final state hadrons, measured by H1 in DIS  $ep$  collisions at high  $Q^2$  in the Breit frame of reference.

*Keywords:* Prompt photons; Charged particle multiplicity; HERA

### 1. Prompt photon production

#### 1.1. Introduction

Isolated high transverse energy photons in the final state are a powerful tool for detailed studies of the Quantum Chromodynamics (QCD) in hard interaction processes and of the hadronic structure of the incoming particles.

The photons are called “prompt” if they are directly coupled to the interacting quarks, instead of being produced as hadronic decay products.

In contrast to jet measurements, where the partonic structure is obscured by the non-perturbative hadronisation process, prompt photons at large transverse energy  $E_T^\gamma$  can be directly related to the partonic event structure. Furthermore, the experimental uncertainties connected with the energy determination of an electromagnetic shower initiated by a photon are smaller compared to the measurement of a hadron jet. However, the cross section for prompt photon production is small and the identification of photons in the detector is not trivial.

Preliminary results for two analyses are presented here: An H1 study of inclusive prompt photons in deep inelastic scattering (DIS)<sup>1</sup>, and a ZEUS study of prompt photons with an accompanying jet

in photoproduction<sup>2</sup>.

#### 1.2. Prompt Photon identification

The main experimental difficulty is the separation of the prompt photons from hadronic background, in particular from signals due to  $\pi^0$  mesons.

In the H1 analysis photons are identified in the liquid argon calorimeter by a compact electromagnetic cluster with no track pointing to it. The photon transverse energy  $E_T^\gamma$  and pseudorapidity  $\eta^\gamma$  are restricted to  $3 \text{ GeV} < E_T^\gamma < 10 \text{ GeV}$  and  $-1.2 < \eta^\gamma < 1.8$ . In order to compare with perturbative QCD (pQCD) calculations, the photon isolation requirement is defined in an infrared-safe way, using:  $z = E^\gamma / E^{\text{photonjet}} > 0.9$ , i.e.  $z$  is the ratio of the photon energy to the energy of the jet, which contains the photon. The photon signal is extracted by a shower shape analysis which uses six discriminating shower shape functions in a likelihood method.

In the ZEUS analysis photons are identified using the barrel preshower detector (BPRES). The BPRES prompt photon signal is determined using the conversion probability in the detector, known from a study of DVCS data<sup>3</sup>.

The photon kinematic range is restricted

to  $5 < E_T^\gamma < 16$  GeV and  $-0.7 < \eta^\gamma < 1.1$ , where positive  $\eta^\gamma$  corresponds to the proton beam direction. The photon isolation criteria are similar to the ones used in the H1 analysis. Hadronic jets were selected in the kinematic range  $6 < E_T^{jet} < 17$  GeV and  $-1.6 < \eta^{jet} < 2.4$ .

### 1.3. Results

Differential cross sections for the production of isolated photons in DIS measured by H1 are shown in Fig. 1, as function of  $E_T^\gamma$  and  $\eta^\gamma$ . A new LO( $\alpha^3$ ) calculation<sup>4</sup> gives a good description, although it lies slightly below the data. At large pseudorapidities the dominant contribution is radiation off the quark line (QQ), whereas in the backward region the radiation off the electron line (LL) dominates the cross section.

A comparison with predictions of the PYTHIA and HERWIG generators (radiation off the quark) plus photon radiation off the electron is also made<sup>1</sup>. Both generators describe the shape in  $E_T^\gamma$  well, but are lower in the absolute scale (factor 2.3 for PYTHIA and 2.6 for HERWIG). The  $\eta^\gamma$  distribution is better described by PYTHIA.

The ZEUS differential cross sections as functions of  $E_T^\gamma$  and  $\eta^\gamma$  for the prompt photons are shown in Fig. 2. Two next-to-order (NLO) pQCD predictions are compared to the data. In both calculations several photon and proton pdf's, and several fragmentation functions are used. The FGH (Fontanaz, Guillet and Heinrich)<sup>5</sup> calculation contains additional higher order corrections to the resolved photon process. Like the KZ (Krawczyk and Zembrzusi)<sup>6</sup> prediction, it describes the data rather well. However, they both underestimate the observed cross section at low  $E_T^\gamma$  and in the backward region. The difference between the data and the NLO QCD calculations is mainly observed in the  $x_\gamma^{obs} < 0.75$  region (not shown), which is sensitive to the resolved photon contribution.

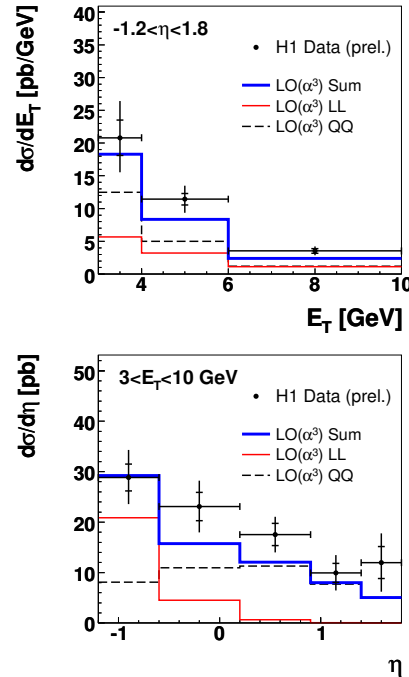


Fig. 1. Prompt photon differential cross sections  $d\sigma/dE_T^\gamma$  for  $-1.2 < \eta^\gamma < 1.8$  and  $d\sigma/d\eta^\gamma$  for  $3 \text{ GeV} < E_T^\gamma < 10 \text{ GeV}$ , for photon virtualities  $Q^2 > 4 \text{ GeV}^2$  and  $y_e > 0.05$ . Curves show an LO calculation with LL and QQ giving the contribution of radiation off the electron and the quark line respectively. As the interference is very small it is not shown, but included in the sum.

A comparison with the prediction of Lipatov and Zotov<sup>7</sup> (LZ), which is based on  $k_T$ -factorisation, corrected for hadronisation effects, is also shown. The LZ prediction gives the best description of the  $E_T^\gamma$  and  $\eta^\gamma$  cross sections. In particular, it describes the lowest  $E_T^\gamma$  region better than the KZ and FGH NLO predictions. PYTHIA and HERWIG do not rise as steeply at low  $E_T^\gamma$  as do the data and underestimate the measured cross section.

Since the largest difference between the NLO calculations and the data is observed in the region of low  $E_T^\gamma$  and low  $\eta^\gamma$ , the level of agreement with NLO QCD was verified by increasing the minimum transverse energy of prompt photons from 5 to 7 GeV.

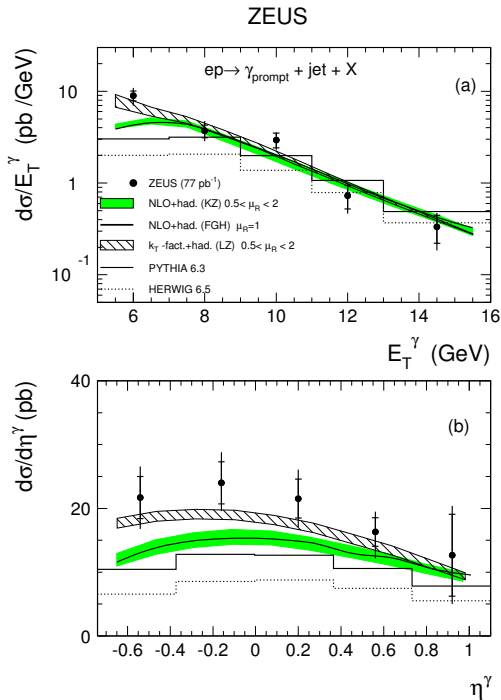


Fig. 2. The differential cross section for the prompt photon events with an accompanying jet as functions of  $E_T^\gamma$  and  $\eta^\gamma$  compared to theoretical QCD calculations (including hadronisation corrections). The shaded bands correspond to the uncertainty in the renormalisation scale which was changed by factors 0.5 and 2.

In this case hadronisation corrections are expected to be smaller. As shown in Fig. 3 with  $E_T^\gamma > 7$  GeV the NLO QCD and the LZ predictions all agree well with the data. The PYTHIA model then also agrees well, while HERWIG is still below the data.

## 2. Charged Particle Momentum distributions

In an H1 analysis<sup>8</sup> the process of parton fragmentation and hadronisation is studied using inclusive charged particle spectra in DIS. In the current region of the Breit frame a comparison with one hemisphere of  $e^+e^-$  annihilation offers a direct possibility to test quark fragmentation universality.

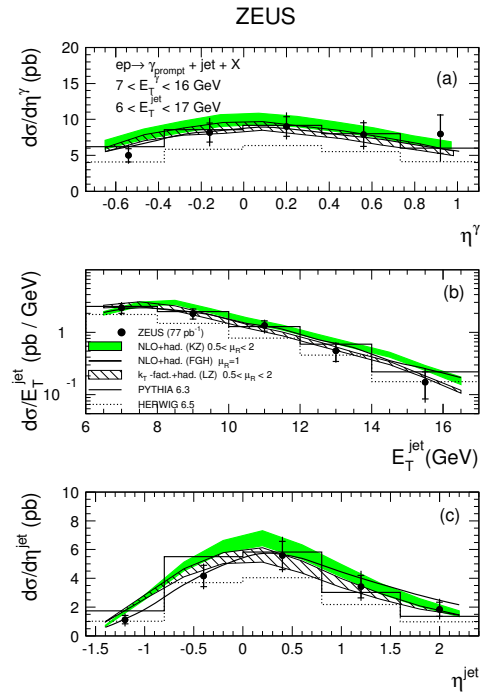


Fig. 3. The differential cross section for the  $\gamma +$  jet events as function of: a)  $\eta^\gamma$ , b)  $E_T^{jet}$  and c)  $\eta^{jet}$  compared to QCD calculations (with hadronisation corrections) and Monte Carlo models. The cut on  $E_T^\gamma$  is increased to 7 GeV.

The energy scale for the current region, set by the virtual photon, is given by  $Q/2$  and, for purpose of comparison, is taken to be equivalent to one half of the  $e^+e^-$  c.m. energy  $E^*/2$ .

In the Breit frame the scaled momentum variable  $x_p$  is defined to be  $2p_h^\pm/Q$ , where  $p_h^\pm$  is the momentum of a charged particle. In  $e^+e^-$  annihilation events the equivalent variable is  $2p_h^\pm/E^*$ .

The use of much higher statistics now available at high  $Q$  as compared to previous studies<sup>9,10</sup>, as well as an improved understanding of the H1 detector and associated systematics, provide a much improved measurement of the scaled momentum spectra. Results are now available up to  $\langle Q \rangle \sim 100$  GeV, close to the LEP-1 c.m. energy, and in

the full range of  $x_p$  ( $0 < x_p < 1$ ).

In Fig. 4 the inclusive, event normalised, charged particle scaled momentum spectrum is shown as a function of  $Q$  for nine different bins of  $x_p$ . Also shown is a comparison to results from  $e^+e^-$  annihilation data (see references in ref. 8). As seen, the  $ep$  and  $e^+e^-$  data are in excellent agreement, which supports the concept of quark fragmentation universality.

Moving from low to high  $Q$  the  $x_p$  spectra become softer, i.e. there is a dramatic increase in the number of hadrons with a small share of the initial parton's momentum and a decrease of those hadrons with a large share. These scaling violations (parton splitting in QCD) are compatible to the scaling violations observed for the DIS structure functions.

In the RAPGAP simulation<sup>11</sup>, also shown in Fig. 4, the Parton Shower model is implemented. It describes the fragmentation process as the splitting of parent partons into two daughters (e.g.  $q \rightarrow qg, q \rightarrow qq, g \rightarrow qq$ ), the splitting continues with daughters going on to form parents. The evolution of the parton shower is based on leading  $\log Q^2$  DGLAP splitting functions. RAPGAP gives a very good description of the  $ep$  scaled momentum spectra over the whole range of  $x_p$ .

## References

1. H1 Coll., A. Aktas *et al.*, Contributed paper to the 33rd International Conference on High Energy Physics, Moscow (2006).
2. ZEUS Coll., S. Chekanov *et al.*, Contributed paper to the 33rd International Conference on High Energy Physics, Moscow (2006).
3. ZEUS Coll., S. Chekanov *et al.*, *Phys. Lett.* **B573**, 46 (2003).
4. A. Gehrmann-De Ridder, T. Gehrmann and E. Poulsen, hep-ph/0601073, 2006; *ibid.* hep-ph/0604030, 2006.
5. M. Fontannaz, J.P. Guillet and G. Heinrich, *Eur. Phys. J.* **C21**, 303 (2001); M. Fontannaz and G. Heinrich, *Eur. Phys. J.* **C34**, 191 (2004).

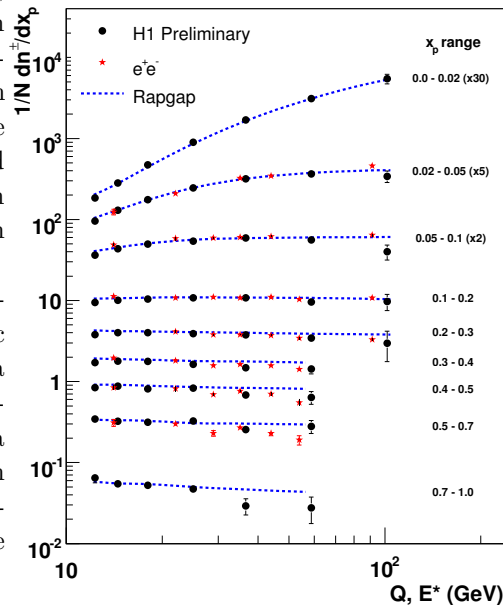


Fig. 4. H1 data for the event normalised inclusive scaled momentum spectrum as a function of  $Q$  for nine different  $x_p$  regions. Also shown are data from various  $e^+e^-$  experiments (taking  $Q = E^*$ ). The DIS data are compared with the RAPGAP generator.

6. M. Krawczyk and A. Zembrzusi, *Phys. Rev.* **D64**, 14017 (2001); A. Zembrzusi and M. Krawczyk, hep-ph/0309308, 2003.
7. A.V. Lipatov and N.P. Zotov, *Phys. Rev.* **D72**, 054002 (2005).
8. H1 Coll., A. Aktas *et al.*, Contributed paper to the 33rd International Conference on High Energy Physics, Moscow (2006).
9. H1 Coll., S. Aid *et al.*, *Nucl. Phys.* **B445**, 3 (1995); H1 Coll., S. Adloff *et al.*, *Nucl. Phys.* **B504**, 3 (1997); H1 Coll., S. Adloff *et al.*, ICHEP98: 29th Int. Conf. on High Energy Physics, Vancouver, 531 (1998)
10. ZEUS Coll., M. Derrick *et al.*, *Z. Phys.* **C67**, 93 (1995); ZEUS Coll., M. Derrick *et al.*, *Phys. Lett.* **B414**, 428 (1997); ZEUS Coll., J. Breitweg *et al.*, *Eur. Phys. J.* **C11**, 251 (1999).
11. H. Jung, *Computer Phys. Comm.* **86**, 147 (1995).